

Provided for non-commercial research and education use.
Not for reproduction, distribution or commercial use.



This article appeared in a journal published by Elsevier. The attached copy is furnished to the author for internal non-commercial research and education use, including for instruction at the authors institution and sharing with colleagues.

Other uses, including reproduction and distribution, or selling or licensing copies, or posting to personal, institutional or third party websites are prohibited.

In most cases authors are permitted to post their version of the article (e.g. in Word or Tex form) to their personal website or institutional repository. Authors requiring further information regarding Elsevier's archiving and manuscript policies are encouraged to visit:

<http://www.elsevier.com/authorsrights>



Contents lists available at ScienceDirect

Gondwana Research

journal homepage: www.elsevier.com/locate/gr

New constraints on the Jurassic–Cretaceous boundary in the High Andes using high-precision U–Pb data



Verónica V. Vennari^a, Marina Lescano^a, Maximiliano Naipauer^a, Beatriz Aguirre-Urreta^a, Andrea Concheyro^a, Urs Schaltegger^b, Richard Armstrong^c, Marcio Pimentel^d, Victor A. Ramos^{a,*}

^a Instituto de Estudios Andinos Don Pablo Groeber, Universidad de Buenos Aires-CONICET, Buenos Aires, Argentina

^b Section of Earth and Environmental Sciences, Université de Genève, Switzerland

^c Research School of Earth Sciences, Australian National University, Canberra, Australia

^d Instituto de Geociências, Universidade Federal do Rio Grande do Sul, Porto Alegre, Brazil

ARTICLE INFO

Article history:

Received 13 December 2012

Received in revised form 7 July 2013

Accepted 21 July 2013

Available online 29 July 2013

Handling Editor: M. Santosh

Keywords:

Nannofossils

Ammonites

U–Pb SHRIMP

U–Pb CA–ID–TIMS

Western Gondwana

ABSTRACT

The Jurassic–Cretaceous (J–K) boundary is poorly constrained, and is the only Phanerozoic system boundary that lacks an internationally accepted reference stratigraphic section (GSSP). Precise radio-isotopic U–Pb data are unavailable for the earliest stage of the Cretaceous—the Berriasian. The age of the Jurassic–Cretaceous boundary was based on several assumptions, including the relative duration of ammonite zones, the constant spreading rates of magnetic anomalies, and the extrapolation of Rb–Sr or K–Ar isotopic data. This paper discusses a site in an Andean Basin of Western Gondwana showing the J–K boundary interval with geographically widespread nannofossil markers which are here uniquely combined with precise radiometric dates. The recent finding of a sequence of marine black shales in the High Andes of Argentina, interbedded with ash-fall tuffs, provides important constraints on this boundary. This succession bears calcareous nannofossils and ammonites, which allow correlation with well-established Tethyan floras and faunas in the northern hemisphere. The Tithonian–Berriasian transition in the Andes was recognized on the basis of ammonite zones and nannofossil bioevents for the first time in the southern hemisphere. The new ages obtained are 137.9 ± 0.9 Ma by sensitive high-resolution ion microprobe (SHRIMP), and $139.55 \pm 0.09/0.18$ Ma by chemical-abrasion isotope-dilution thermal ionization mass spectrometry (TIMS) near the base of the Berriasian. These new ages can be interpreted in two different ways. The first alternative would indicate that the present geological time table is correct and the fossil levels should be late Berriasian. The second alternative is that the J–K boundary is 5 Ma younger than the recently published geological time scale. The authors support the last alternative and propose that the J–K boundary should be close to 140 Ma.

© 2013 International Association for Gondwana Research. Published by Elsevier B.V. All rights reserved.

1. Introduction

The Jurassic–Cretaceous (J–K) boundary as defined by the IUGS International Commission on Stratigraphy (International Stratigraphic Chart, 2012; see also Gradstein et al., 2012) is one of the most problematic of all the system boundaries (Rawson, 2000; Wimbledon et al., 2011). In particular, thin sedimentary sequences in the classical Tethys localities of the northern Hemisphere, which contain ammonites, calcareous nannofossils, and calpionellids, have no precise absolute geochronological control. The age of the boundary was historically established based on glauconite dating of sedimentary deposits (Odin, 1982), statistical analyses, and linear interpolations of the duration of ammonite zones with magnetic polarity chrons (Ogg, 2004). According to Pálffy (1995) a more accurate age of this boundary can be achieved only with precise isotopic data, with statistical data analyses and interpolations being

regarded as tools of secondary importance. Later, Mahoney et al. (2005) presented Ar–Ar dating from ocean-floor basalts, combined with calcareous nannofossil and radiolarian biostratigraphy for the J–K boundary. High precision U–Pb dating of volcanic tuffs intercalated with fossiliferous sediments in Late Jurassic–Early Cretaceous sequences is more valuable because the K–Ar system in glauconite is generally unreliable and may yield anomalously young ages (Gradstein et al., 1994). U–Pb methods using only single-zircon analyses by CA–TIMS dating (which must follow treatments of annealing followed by chemical abrasion) are urgently needed according to Gradstein et al. (2012). However, up to now the recalibrated age of ^{40}Ar – ^{39}Ar 145.5 ± 0.8 Ma (Mahoney et al., 2005) has been taken as the most reliable age for the J–K boundary (Ogg and Hinnov, 2012).

The Mesozoic Andean ammonite fauna of Western Gondwana has historically been correlated with typical Tethyan assemblages. In particular, the Jurassic–Early Cretaceous ammonite zonation in the Neuquén Basin of west central Argentina, through more than a century of paleontological studies, shows a correlation not only with the northern

* Corresponding author. Tel.: +54 11 4576 3400.

E-mail addresses: andes@gl.fcen.uba.ar, victor@ramos.net (V.A. Ramos).

hemisphere but also all along the Circum-Pacific realm (Leanza, 1981; Riccardi, 1991, 2008; Riccardi et al., 1992; Aguirre-Urreta et al., 2005, 2007, 2008a,b).

Besides, recent studies on calcareous nannofossils in the Neuquén Basin (Scasso and Concheyro, 1999; Ballent et al., 2004; Bown and Concheyro, 2004; Concheyro et al., 2007; Kietzmann et al., 2011) allow correlations with several proposed biozonations in the northern hemisphere (Bralower et al., 1989; Casellato, 2010; Wimbledon et al., 2011).

The aims of this study are threefold: 1) to present an ammonite and nannofossil biostratigraphic zonation of the Late Tithonian–Early Berriasian in the Neuquén Basin; 2) to date an ash-fall tuff layer associated with this marine sequence using SHRIMP and CA-ID-TIMS U–Pb dating in zircons; and 3) to propose a numerical age of the J–K boundary from the High Andes based on these high precision dates combined with LAM-MC-ICP-MS U–Pb detrital zircon ages of underlying continental deposits.

2. Geological setting

The Neuquén Basin is located in the foothills of the Andes as a retroarc basin developed in a normal subduction segment (Jordan et al., 1983). As such it has an almost continuous record of volcanic activity, which is associated with more than 6000 m of sediments whose complex depositional history was mainly controlled by changing tectonic regimes along the western margin of Gondwana (Ramos and Folguera, 2005). The Mesozoic stratigraphy has been established through a series of classic studies, beginning in the 19th century, and numerous subsequent contributions that made the Neuquén Basin one of the best known Andean basins of South America (see Gulisano et al., 1984; Legarreta and Uliana, 1991, 1999; Veiga et al., 2005). The abundant and well preserved fossils are the subject of many monographs and important studies on its invertebrate fauna and flora (Riccardi, 1988, 1991; Aguirre-Urreta and Rawson, 1997; Bown and Concheyro, 2004; Aguirre-Urreta et al., 2005, 2011).

Our work focuses on exposures of Tithonian–Berriasian black shales of the Vaca Muerta Formation in the Las Loicas section of the northern Neuquén Basin, situated in the High Andes of southern Mendoza, Argentina. In the early Tithonian, a major transgression associated with a sea-level rise was linked to fast subsidence and strong expansion of the marine area, which deposited the Vaca Muerta Formation (Legarreta and Uliana, 1999). These shales are interbedded with ash-fall tuffs, and bear ammonites and other associated fauna and calcareous nannofossils. Due to the proximity to the magmatic arc located at

that time on the Chilean slope of the Andes, tuff horizons are intercalated with sediments for which a precise biozonation is available. This work is part of a broad interdisciplinary program aimed at producing a high-precision biostratigraphy and absolute geochronology for the Late Jurassic–Early Cretaceous marine deposits of the Neuquén Basin (Aguirre-Urreta et al., 2008b).

The Las Loicas section is exposed along a road that forks from national road 145, from Bardas Blancas to the international border at Pehuenche Pass. It is located near the Argentine–Chilean border, approximately 1 km to the southwest of the settlement Las Loicas, 34 km west of Bardas Blancas (Figs. 1 and 2). The 217 m thick section of marine black shales and mudstones of the Vaca Muerta Formation at Las Loicas spans an interval from the upper Lower Tithonian (*Virgatosphinctes mendozanus* biozone) to the Upper Berriasian (*Spiticeras damesi* biozone). This succession conformably overlies a thick pile of fluvial red sandstones, conglomerates and green siltstones of the Tordillo Formation (Spalletti and Piñol, 2005; Veiga and Spalletti, 2007). The section is exposed on the western flank of a gentle dipping anticline. The middle section of the Vaca Muerta Formation is partially covered by a minor landslide. Thus, our detailed analysis is restricted to the upper part of the section, as shown in Fig. 3.

3. Material and methods

The Las Loicas section of the Vaca Muerta Formation was measured bed by bed, and systematic sampling was done in order to study the mega, micro and nannofossil contents. However, the black shales analyzed for dinoflagellates gave negative results, probably due to high thermal alteration related to the burial of Vaca Muerta Formation while the limestones did not yield calpionellids, a group represented by very few records in the basin. So, our biostratigraphic study concentrates in ammonites and nannofossils.

3.1. Nannofossils

Out of the 60 samples from the Las Loicas section of the Vaca Muerta Formation that were examined for calcareous nannofossils, 45 were fossiliferous. Samples were prepared on smear slides using standard techniques. Systematic determinations were established by a standard LEICA DMLP microscope, under 1000× magnification, crossed Nicols and a gypsum plate. The range chart (Table 1) indicates the nannoflora distribution recognized in each level; the barren samples are also considered. The fossiliferous ones were placed in the Department of

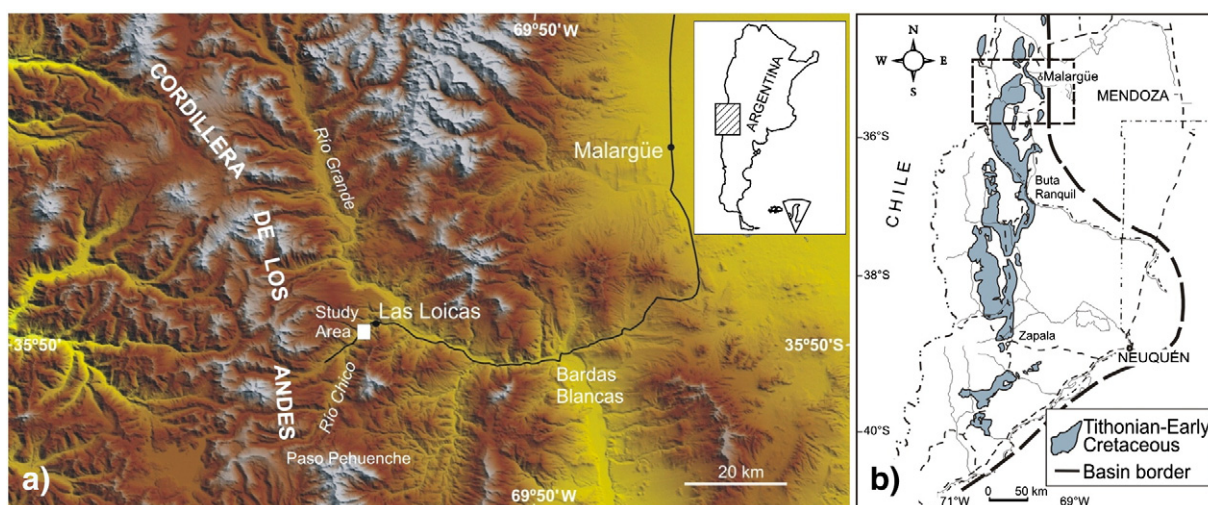


Fig. 1. a) Location map of the Las Loicas section in the High Andes of southern Mendoza with the main access road; b) Outline of the Neuquén Basin with main outcrops of Tithonian–Early Cretaceous age with indication of the study area.

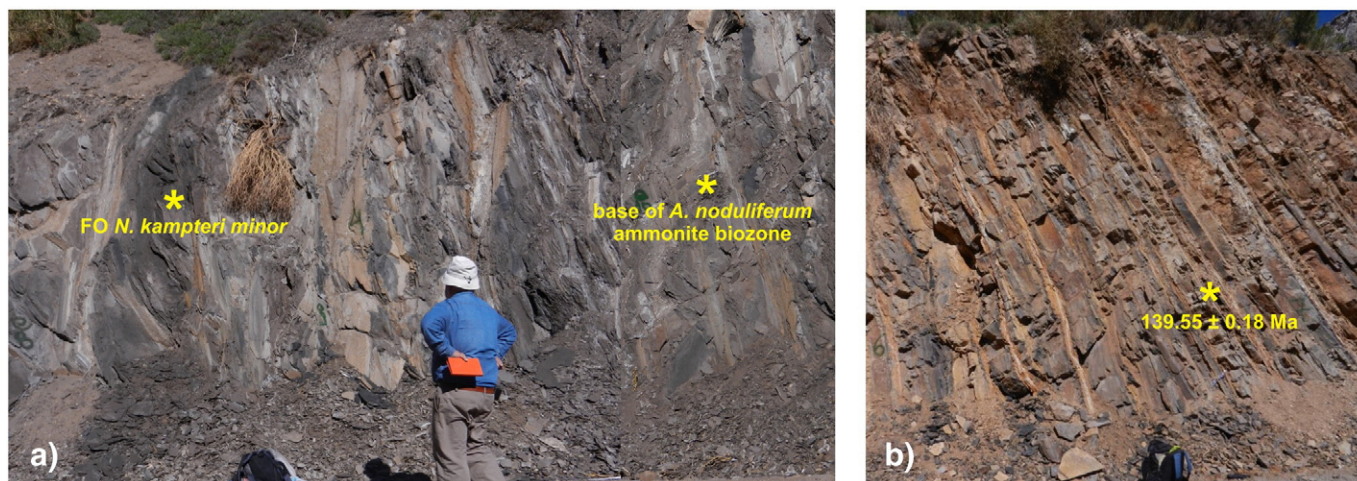


Fig. 2. View of Vaca Muerta Formation in the Las Loicas section: a) location of the first occurrence of *Nannoconus kamptneri minor* and the base of *Argenticeras noduliferum* ammonite biozone, which were used to constrain the J–K biostratigraphic boundary in the Andes; b) location of the dated tuff.

Geological Sciences, University of Buenos Aires, under the acronym BACF-NP 3850-3908.

3.2. Ammonites

The Vaca Muerta Formation in Las Loicas section yielded more than 450 ammonites from fifty-four levels. Most of the specimens are well preserved as impressions, but three-dimensional casts have also been recovered. In both taphonomic modes, ornamentation features and mature apertural modifications, which are very helpful in identifying sexual dimorphism, can be observed. Figured ammonoids are housed at the Repositorio de Paleontología del Museo de Ciencias Naturales y Antropológicas Juan Cornelio Moyano, Mendoza Province, Argentina, under the numbers MCNAM-PI 24551-24557.

3.3. SHRIMP analyses

Zircon grains were analyzed at the Australian National University in Canberra. Zircon grains were mounted in epoxy disks, polished and studied with cathodoluminescence to determine their morphology and internal structure. Based on the cathodoluminescence images, 24 zircon grains were selected for analysis with a SHRIMP II ion microprobe (Supplementary Table 1). The AS3 zircon standard (1099 Ma; $^{206}\text{Pb}/^{238}\text{U} = 0.1859$) was used for calibration purposes. Data were processed in a manner similar to that described in Williams and Claesson (1987).

3.4. CA-ID-TIMS analyses

Single zircons were picked for chemical abrasion (Mattinson, 2005) and combined in a quartz beaker for annealing at 900 °C for ~60 h. All grains from a single sample were leached together in 3 ml Savillex beakers in HF + trace HNO₃ for ~12 h, rinsed with water and acetone and then placed in 6 N HCl on a hotplate at ~110 °C overnight. These were then washed several times with water, HCl and HNO₃. Single grains were then handpicked for dissolution. Each grain was spiked with ~0.004 g of the EARTHTIME ^{202}Pb - ^{205}Pb - ^{233}U - ^{235}U tracer solution. Zircons were dissolved in ~70 μl 40% HF and trace HNO₃ in 200 μl Savillex capsules at 210 °C for >48 h, dried and redissolved in 6 N HCl overnight. Samples were then dried and redissolved in 3 N HCl and put through a modified single 50 μl column anion exchange chemistry. U and Pb were collected in the same beaker for zircon, dried with a drop of 0.05 M H₃PO₄. They were analyzed on a single outgassed Re filament in a Si-gel emitter modified from (Gerstenberger and Haase,

1997). Measurements were performed on a Thermo-Finnigan Triton thermal ionization mass spectrometer at the University of Geneva.

Pb was measured in dynamic mode on a modified MasCom secondary electron multiplier (SEM). The deadtime for the SEM was determined by periodic measurement of NBS-982 for up to 1.3 Mcps and observed to be constant at 23.5 ns. Multiplier linearity was monitored every few days between 1.3×10^6 and <100 cps by a combination of measurements of NBS-981, -982 and -983 and observed to be constant if the Faraday-to-SEM yield was kept between ~93 and 94% by adjusting the SEM voltage. Interferences for ^{202}Pb and ^{205}Pb were monitored by measuring masses 201 and 203, but no corrections were applied. Mass fractionation was corrected using the EARTHTIME ^{202}Pb - ^{205}Pb - ^{233}U - ^{235}U tracer, and each measured ratio was corrected for fractionation in the data acquisition software using a $^{202}\text{Pb}/^{205}\text{Pb}$ of 0.99989, giving an average Pb fractionation of $0.13 \pm 0.04\%$ a.m.u. (2 σ standard deviations).

U was measured in static mode on Faraday cups and $10^{12} \Omega$ resistors as UO_2^+ . Baselines were measured at ± 0.5 mass units for 30 s every 50 ratios. Correction for mass-fractionation for U was performed with the double spike, assuming a sample $^{238}\text{U}/^{235}\text{U}$ ratio of 137.88. Measured ratios were reduced using an integrated open-source infrastructure, interfaced with commercial mass spectrometers for read-out and statistical filtering of the raw data (“Tripoli”), followed by a platform allowing for data reduction, correct uncertainty propagation and online data visualization (“U–Pb Redux”, Bowring et al., 2005; McLean et al., 2011). A tracer $^{235}\text{U}/^{205}\text{Pb}$ of 100.23 was used, to which a total uncertainty of 0.1 was assigned. All common Pb found in the analysis was considered to come from the blank, with the following isotope composition: $^{206}\text{Pb}/^{204}\text{Pb} = 18.39 \pm 0.22$, $^{207}\text{Pb}/^{204}\text{Pb} = 15.62 \pm 0.20$, and $^{208}\text{Pb}/^{204}\text{Pb} = 37.62 \pm 0.78$ (2 σ standard deviations) (Supplementary Table 2).

3.5. LAM-MC-ICP-MS analyses

Heavy mineral concentrates were obtained using conventional gravimetric and magnetic techniques; the final purification was achieved by hand picking under a binocular microscope. Selected zircon grains were mounted on an epoxy mount. The mount surface was then polished to expose the grain interiors. Backscattered electron images of zircons were obtained using an SEM JEOL JSM 5800 at Universidade Federal do Rio Grande do Sul, Brazil, following the procedures described in Matteini et al. (2010). Prior to LA-ICP-MS analysis, the mounts were cleaned by carefully rinsing with dilute (2%) HNO₃. Once fully dry, the samples were mounted in a laser cell specially adapted for thick sections, loaded into an UP 213 neodymium-doped yttrium aluminum

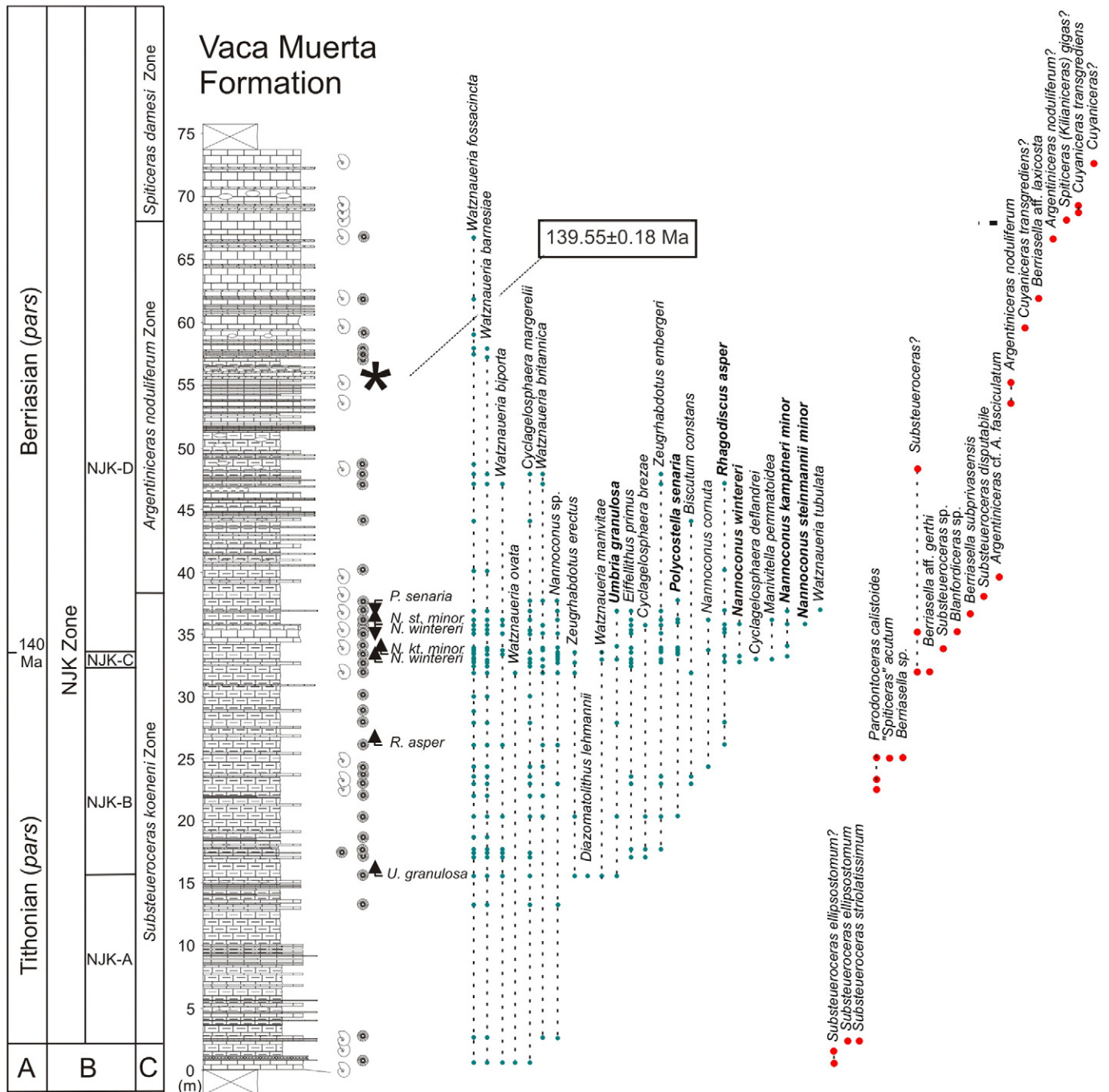


Fig. 3. Upper part of the Vaca Muerta Formation at the Las Loicas section: lithostratigraphy and nannofossil and ammonite distribution. A, proposed boundary; B, calcareous nannofossil zone and subzones after Bralower et al. (1989); C, ammonite zones after Leanza (1981).

garnet laser ($\chi = 213$ nm), and linked to a multi-collector, high-resolution Neptune ICP–MS.

4. Results

4.1. Nannofossils

The recovered nannoflora presents low richness, moderate to poor preservation and is mainly dominated by abundant watznauerids, such as *Watznaueria fossacincta*, *Watznaueria barnesiae*, *Watznaueria ovata*, *Watznaueria biporta*, and *Cyclagelosphaera margerelii*. Other species include *Nannoconus kamptneri minor*, *Nannoconus wintereri*, *Nannoconus steinmanni minor*, *Manivitella pemmatoidea*, *Diazomatholithus*

lehmannii, *Biscutum constans*, *Umbria granulosa*, *Zeughrabdotus embergeri*, *Zeughrabdotus erectus*, *Polycostella senaria*, *Eiffelithus primus* and *Rhagodiscus asper* (Fig. 4). A complete list of calcareous nannofossil species is shown in Table 1.

Bralower et al. (1989) proposed a calcareous nannofossil zonation for the Jurassic and Cretaceous based on southern European land sections and the western North Atlantic, DSDP Sites 391C and 534A. In particular, the NJK biozone straddled the Tithonian–Berriasian boundary. They subdivided the NJK biozone into four subzones NJK–A, NJK–B, NJK–C and NJK–D, marking their boundaries with secondary bioevents such as the first occurrences (FADs) of *Microstaurus chiastius*, *Umbria granulosa granulosa*, *Rotellapillus laffitei* and *Nannoconus steinmanni minor*, respectively (see Fig. 5). These authors placed the base of the

Table 1
Stratigraphic distribution of calcareous nannofossils of Las Loicas section and list of calcareous nannofossil species in alphabetical order by generic epithets.

Samples	<i>Watznaueria fossacincta</i>	<i>Watznaueria barnesiae</i>	<i>Watznaueria biporta</i>	<i>Watznaueria ovata</i>	<i>Cyclagelosphaera margerelli</i>	<i>Watznaueria britannica</i>	<i>Nannoconus sp.</i>	<i>Zeugrhabdotus erectus</i>	<i>Watznaueria manivitae</i>	<i>Diazomatolithus lehmanni</i>	<i>Umbria granulosa</i>	<i>Cyclagelosphaera brezae</i>	<i>Eiffelithus primus</i>	<i>Zeugrhabdotus embergeri</i>	<i>Polycostella senaria</i>	<i>Biscutum constans</i>	<i>Nannoconus cornuta</i>	<i>Rhagodiscus asper</i>	<i>Nannoconus wintereri</i>	<i>Cyclagelosphaera deflandrei</i>	<i>Manivitella pemmatoidea</i>	<i>Nannoconus kamptneri minor</i>	<i>Nannoconus steinmannii minor</i>
3909	X																						
3908																							
3907	X																						
3906																							
3905																							
3904																							
3903	X																						
3902																							
3901	X	X																					
3900	X																						
3899		X																					
3898																							
3897																							
3896																							
3895																							
3894	X																						
3893	X	X			X	X							X										
3892	X	X	X			X							X					X					
3891																							
3890	X				X										X								
3889	X	X																X					
3888																							
3887																							
3886					X	X	X								X								
3885	X	X			X		X				X	X	X					X				X	
3884	X	X	X		X		X					X	X	X		X				X			
3883															X				X		X	X	
3882	X	X	X		X	X	X						X	X				X					
3881	X	X	X			X						X	X	X				X					
3880	X	X			X								X	X				X					
3879											X												X
3878	X	X				X	X						X	X	X								
3877	X	X	X			X	X						X	X			X						
3876	X				X		X	X					X	X	X		X						
3875	X	X	X				X								X								
3874	X						X											X	X			X	
3873	X	X			X	X	X		X				X	X						X	X		
3872	X	X			X		X	X					X	X				X	X				
3871	X	X			X	X							X										
3870	X	X		X		X	X	X							X								
3869																							
3868	X	X			X																		
3867	X																						
3866	X	X			X						X							X					
3865																							
3864	X	X	X			X	X											X					
3863	X	X			X	X											X						
3862	X	X			X								X	X		X							
3861	X	X			X		X						X	X		X							
3860	X	X			X	X																	
3859	X	X	X		X	X		X			X	X		X	X								
3858	X	X																					
3857																							
3856	X	X	X	X								X	X	X									
3855	X	X	X		X																		
3854	X	X	X		X							X	X										
3853	X	X	X		X			X	X	X	X												
3852	X	X			X		X																
3851	X	X				X	X																
3850	X	X	X	X	X																		

X Calcareous nannofossil event Barren sample

Biscutum constans (Górka) Black
Cyclagelosphaera brezae Applegate and Bergen
Cyclagelosphaera deflandrei (Manivit) Roth
Cyclagelosphaera margerelli Noël
Cyclagelosphaera sp.
Diazomatolithus lehmanni Noël
Eiffelithus primus Applegate and Bergen
Manivitella pemmatoidea (Deflandre)
Thierstein
Nannoconus cornuta Deres Achéritéguy and
Nannoconus kamptneri minor Bralower
Nannoconus sp.
Nannoconus steinmannii minor Deres and
Achéritéguy
Nannoconus wintereri Bralower and
Thierstein
Polycostella senaria Thierstein
Rhagodiscus asper (Stradner) Reinhardt
Umbria granulosa Bralower and Thierstein
Watznaueria barnesiae (Black) Perch-
Nielsen
Watznaueria biporta Bukry
Watznaueria britannica (Stradner)
Reinhardt
Watznaueria fossacincta (Black) Bown
Watznaueria manivitae Bukry
Watznaueria ovata Bukry
Watznaueria tubulata (Grün Zweili) de and
Kaenel and Bergen
Zeugrhabdotus embergeri (Noël) Perch-
Nielsen, 1984
Zeugrhabdotus erectus (Deflandre)
Reinhardt, 1965
Zeugrhabdotus sp.

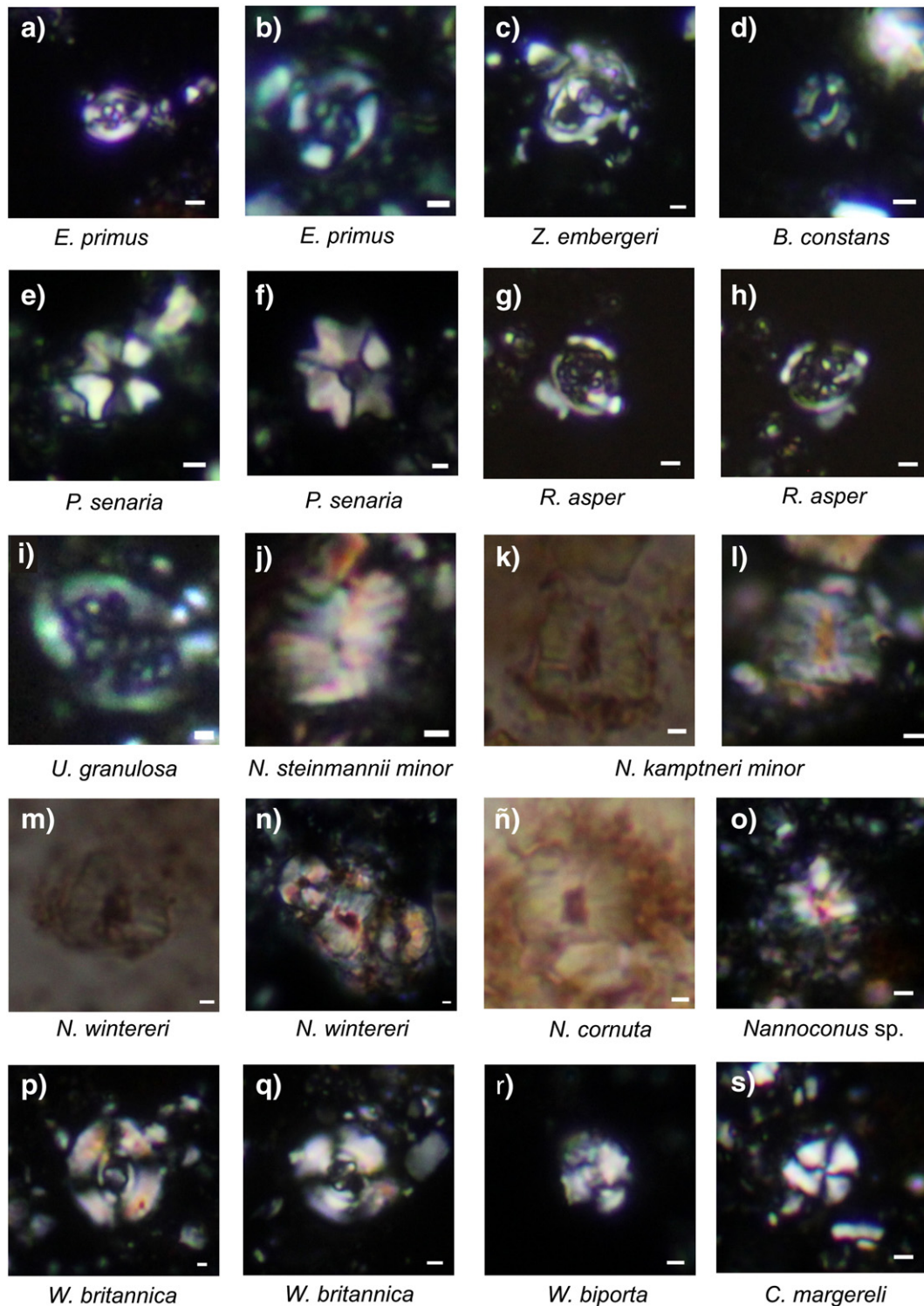


Fig. 4. Calcareous nannofossil from the Las Loicas section. All photomicrographs under crossed nicols (polarized light), white bar = 1 μm . a–b) *Eiffellithus primus* Applegate and Bergen. c) *Zeugrhabdotus embergeri* (Noël) Perch-Nielsen. d) *Biscutum constans* (Görka) Black. e–f) *Polycostella senaria* Thierstein. g–h) *Rhagodiscus asper* (Stradner) Reinhardt. i) *Umbria granulosa* Bralower and Thierstein. j) *Nannoconus steinmannii minor* Deres and Achéritéguy. k–l) *Nannoconus kamptneri minor* Bralower. m–n) *Nannoconus wintereri* Bralower and Thierstein. ñ) *Nannoconus cornuta* Deres y Achéritéguy. o) *Nannoconus* sp. p–q) *Watznaueria britannica* (Stradner) Reinhardt. r) *Watznaueria biporta* Bukry. s) *Cyclagelosphaera margereli* Noël.

Berriasian in the middle of their subzone NJK–C, which coincided with the base of magnetochron M18, the base of the ammonoid biozone of *Berriasella jacobii* and the base of the calpionellid biozone of *Calpionella alpina*. Besides, Bralower et al. (1989) correlated their biozones with other bioevents such as the FAD of *Rhagodiscus asper* and *Nannoconus wintereri*.

More recently, Casellato (2010) proposed a new calcareous nannofossil biostratigraphic scheme for the Tithonian–Early Berriasian

established for the Southern Alps in Northern Italy. She defined the biozones NJT 16, NJT 17 and NKT on the basis of FAD of *Helenea chiastia*, *Nannoconus globulus minor* and *Nannoconus steinmannii minor* and placed the base of the Berriasian coinciding with the base of NKT biozone (i.e. FAD of *N. steinmannii minor*).

Six calcareous nannofossil markers previously identified in Tethyan samples (Bralower et al., 1989; Casellato, 2010) were recognized in

AGE			Bralower et al. (1989)	Casellato (2010)	Other authors	Previous studies Neuquén Basin	This study
CRETACEOUS	Berriasian	Early	NK-1 <i>N. steinmannii steinmannii</i> FAD <i>N. steinmannii steinmannii</i>	FAD <i>N. steinmannii steinmannii</i>	▲ <i>N. kamptneri kamptneri</i> (2, 5, 9) ▲ <i>C. cuvillieri</i> (1, 7) ▲ <i>C. octofenestrata</i> (9)	<i>M. hoschulzii</i> (8)	▼ <i>P. senaria</i>
		Late	NJK <i>Microstaurus chiastrus</i>	NKT FAD <i>N. steinmannii minor</i>	▲ <i>N. kamptneri minor</i> (2, 10) ▲ <i>R. surrella</i> (7) ▲ <i>S. colligata</i> (2, 9)		▲ <i>N. steinmannii minor</i> ▲ <i>N. wintereri</i> ▲ <i>N. kamptneri minor</i> ▲ <i>N. wintereri</i>
JURASSIC	Tithonian	Early	NJK-A <i>H. noeliae</i> FAD <i>Microstaurus chiastrus</i>	NJT 17b FAD <i>N. wintereri</i>	▲ <i>R. asper</i> (2, 5, 9) ▲ <i>M. permatoidea</i> (3) ▼ <i>P. beckmannii</i> (2) ▲ <i>N. globulus</i> (9) ▲ <i>L. carniolensis</i> (2)		▲ <i>R. asper</i>
		Late	NJK-B <i>U. granulosa granulosa</i> FAD <i>U. granulosa granulosa</i>	NJT 17a FAD <i>N. globulus minor</i>	▲ <i>N. puer</i> (12) ▲ <i>M. ellipticus</i> , <i>E. primus</i> (3)	<i>P. senaria</i> (6) <i>P. beckmannii</i> (4)	▲ <i>U. granulosa</i>
		Early	NJ-20 <i>Conusphaera mexicana</i>	NJT 16a FAD <i>H. chiastris</i> , <i>H. noeliae</i> y <i>P. senaria</i>	▲ <i>N. compressus</i> (2, 5)	<i>P. senaria</i> (11)	
			NJK-C <i>R. laffittei</i> FAD <i>R. laffittei</i>				
			NJK-D <i>N. steinmannii minor</i> FAD <i>N. steinmannii minor</i>				
			NJ-20B <i>P. beckmannii</i> FAD <i>P. beckmannii</i>				

Fig. 5. Correlation chart of Tithonian–Early Berriasian calcareous nannofossils biostratigraphy with bioevents recognized in the literature and in this study. In the column other authors the numbers in brackets correspond to: 1) Thierstein, 1971; 2) Bralower et al., 1989; 3) de Kaenel and Bergen, 1996; 4) Scasso and Concheyro, 1999; 5) Bornemann et al., 2003; 6) Ballent et al., 2004; 7) Kessel et al., 2006; 8) Concheyro et al., 2007; 9) Casellato, 2009; 10) Wimbledon et al., 2011; 11) Kietzmann et al., 2011; 12) Channell et al., 2010.

the studied section, here spanning the Late Tithonian to the Early Berriasian (Fig. 5). Tethyan NJK zone has been established and its NJK–A, NJK–B, NJK–C and NJK–D subzones confined to the studied interval. The FAD of *Umbria granulosa* is considered the principal event of subzone NJK–B and correlated with the uppermost Tithonian. The appearance of *Rhagodiscus asper* is a secondary bioevent (Casellato, 2010) and a further marker for the upper part of subzone NJK–B (Bralower et al., 1989). Another Late Tithonian marker is the FAD of *Nannoconus wintereri*, a bioevent of subzone NJK–C (Bralower et al., 1989), and defines the base of Subzone NJT 17 b (Casellato, 2010). The FAD of *Nannoconus kamptneri minor* defines the base of subzones NJK–D (Bralower et al., 1989) and NKT (Casellato, 2010), assigned to the Berriasian. Currently, this event is considered a reliable marker of the Tithonian–Berriasian boundary (Michalík and Reháková, 2011; Wimbledon et al., 2011). *Polycostella senaria* constitutes an important Late Tithonian nannofossil marker, which has previously been noted in the Vaca Muerta Formation in the Entre Lomas area, Neuquén and Río Negro provinces (Ballent et al., 2004) and in the Loncoche area, Mendoza province (Kietzmann et al., 2011). This species is very resistant to dissolution and its stratigraphic range is restricted to the Middle–Late Tithonian to Early Berriasian interval. In the study section, the last occurrence (LOD) of *Polycostella senaria* and *Nannoconus wintereri* and the FAD of *Nannoconus steinmannii minor* confirm the Berriasian age.

The base of the section, placed in the NJK–A nannofossil subzone, is mainly composed of watznauerids. From the base of NJK–B subzone the richness increases, spanning the NJK–C subzone. Above the J–K boundary, in the NJK–D nannofossil subzone, nannoliths are frequent, including the representatives *P. senaria*, *N. kamptneri minor* and *N. wintereri* (Fig. 5). Higher in the section, in the NJK–D nannofossil subzone, the richness diminishes progressively, and the association becomes extremely poor; this subzone is represented by specimens of *W. fossacincta* and *W. barnesiae*.

4.2. Ammonites

Six Tithonian and two Berriasian ammonite assemblage zones have been recognized in the Las Loicas section, based on abundant material

and following the classic Andean biostratigraphic scheme (Leanza, 1981; Riccardi, 1988; Aguirre-Urreta et al., 2005) and its recent modification (Zeiss and Leanza, 2010). The Mediterranean standard zones–Tithonian zones after Ogg et al. (2008) and Berriasian after Reboulet et al. (2011) – are correlated with Andean biozones as shown in Fig. 6.

	Stage	Andean Zones	Tethys/Mediterranean Zones
BERRIASIAN	Late	<i>Spiticeras damesi</i>	<i>Subthurmannia boissieri</i>
	Middle	<i>Argentiniceras noduliferum</i>	<i>Subthurmannia occitanica</i>
	Early	<i>Substeuerocheras koeneri</i>	<i>Berriasella jacobi</i>
TITHONIAN	Late	<i>Corongoceras alternans</i>	<i>Durangites</i>
		<i>Windhauseniceras internispinosum</i>	<i>Micracanthoceras microcanthum</i>
		<i>Aulacosphinctes proximus</i>	<i>Micracanthoceras ponti/ Burckhardtceras peroni</i>
	Middle	<i>Pseudolissoceras zitteli</i>	<i>Semiformiceras fallauxi</i>
		<i>Virgatosphinctes mendozanus</i>	<i>Semiformiceras semiforme</i>
	Early		<i>Semiformiceras darwini</i>
			<i>Hybonoticeras hybonotum</i>

Fig. 6. Ammonoid biostratigraphy of the Andean Region and its tentative correlation with the Tethys/Mediterranean Region. Andean Tithonian biozonation after Zeiss and Leanza (2010) and Riccardi (2008), Berriasian biozonation after Aguirre-Urreta et al. (2007). Tethys/Mediterranean biozonation after Gradstein et al. (2012) and Reboulet et al. (2011)



Fig. 7. Ammonoids from Las Loicas Section, Mendoza, Argentina. a. *Parodontoceras calistoides* (Behrendsen), MCNAM-PI 24551; b. “*Spiticeras*” *acutum* Gerth MCNAM-PI 24552; c. *Berriasella subprivasensis* (Krantz) MCNAM-PI 24553a; d–e. *Substeueroceras striolatissimum* (Steuer) MCNAM-PI 24554–24555; f. *Argentineroceras noduliferum* Leanza MCNAM-PI 24556; g. *Cuyaniceroceras transgrediens* (Steuer), MCNAM-PI 24557; a–e: *Substeueroceras koeneni* Assemblage Zone (Uppermost Tithonian); f: *Argentineroceras noduliferum* Assemblage Zone (Lower–Middle Berriasian); g: *Spiticeras damesi* Assemblage Zone (Upper Berriasian). Specimens covered with ammonium chloride, white bar = 1 cm.

The upper part of the section, which has been studied in detail, focused on the identification of the three upper assemblage zones: *Substeueroceras koeneni*, *Argentineroceras noduliferum* and *Spiticeras damesi*.

The *Substeueroceras koeneni* assemblage zone was defined by Gerth (1921) and placed in the topmost Tithonian (Leanza, 1945) after the association of its key fossils, *S. koeneni* (Steuer) and *Parodontoceras calistoides* (Behrendsen), with typical Tithonian genera such as *Aspidoceras* (now *Schaireria*) and *Micracanthoceras* (now *Blanfordiceras* pars.). This zone includes species of *Substeueroceras*, *Parodontoceras*, *Blanfordiceras*, *Berriasella*, *Aulacosphinctes*, *Pectinatites* (?), *Himalayites*, “*Spiticeras*” and *Schaireria*. In the Las Loicas section, the zone is represented by *P. calistoides* (Fig. 7a), “*Spiticeras*” *acutum* Gerth (Fig. 7b), *Berriasella subprivasensis* Krantz (Fig. 7c), *Substeueroceras ellipsostomum*

(Steuer), *Substeueroceras striolatissimum* (Steuer) (Fig. 7d–e), *Blanfordiceras* sp. and *Berriasella* sp. aff. *Berriasella gerthi*.

The *Argentineroceras noduliferum* assemblage biozone was proposed in southern Mendoza and placed in the Lower Berriasian (Leanza, 1945). It includes several species of *Argentineroceras*, representatives of *Groebericeras*, *Frenguelligeras*, *Berriasella*, “*Thurmanniceras*”; and some relictual *Substeueroceras*. In the studied section, this zone is represented by *Argentineroceras* sp. cf. *Argentineroceras fasciculatum* (Steuer), *A. noduliferum* (Steuer) (Fig. 7f), *Berriasella* sp. aff. *Berriasella laxicosta* (Steuer) and *Substeueroceras disputabile* Leanza. A few specimens that can be assigned to *Cuyaniceroceras transgrediens*? (Steuer) of the next zone have also been noticed. The beginning of the *A. noduliferum* zone is established where the first occurrence of *S. disputabile* takes place. This

species is found in close association with *Argentinerias* in nearby localities in southern Mendoza (Leanza, 1945), while in the Las Loicas section, it is documented 1.5 m below the first occurrence of *Argentinerias* representatives.

Finally, the *Spiticeras damesi* assemblage biozone was established by Gerth (1921) and placed in the Upper Berriasian by Leanza (1945). It typically includes several species of *Spiticeras* and *Cuyanicerias*, along with representatives of *Neocosmoceras*, *Neocomites*, “*Thurmannicerias*” and *Blanfordicerias*. In the Las Loicas section, this zone is represented by *Spiticeras (Kilianicerias) gigas?* Leanza, *Cuyanicerias transgrediens* (Fig. 7g) and *Cuyanicerias* sp.

The *Substeueroeras koeneni* ammonite zone, traditionally ascribed to the late Tithonian, may reach the early Berriasian according to Riccardi (2008, p. 332), but this proposal was based on unconvincing evidence (Aguirre-Urreta et al., 2011). The changes in the age of the ammonite zone, first introduced by Leanza (1996) and then adopted by Riccardi et al. (2000) and Riccardi (2008) have been based on two misconceptions: (1) that the species *Schaireria longaeva* (Leanza) is of Berriasian age in Argentina; and (2) that “*Spiticeras*” *acutum* Gerth is a probable forerunner of the Berriasian genus *Groebericeras* (Leanza, 1996, p. 216). The first statement is the result of a misinterpretation of Checa (1985, p. 204) of the age of *S. longaeva* in the Neuquén Basin which has been originally established as Late Tithonian by Leanza (1945, p. 26, and associated stratigraphic chart). This mistake was pointed out by Cantú-Chapa (2006, p. 299). The second statement about the close phylogenetic relationship of “*Spiticeras*” *acutum* and *Groebericeras* has not yet been proved and the recombination of “*Spiticeras*” *acutum* to the Tithonian genus *Pronicerias* is currently under evaluation. Besides, being *Groebericeras* a Berriasian genus associated with *Argentinerias* in the Neuquén Basin, having a forerunner of Tithonian age would still be valid and it is not necessary to move higher up the *Substeueroeras* zone.

The placement of the *S. koeneni* zone into the early Berriasian as envisaged by Zeiss (1983, p. 431, 1986, p. 28) is the result of an indirect correlation of the Argentinian *Substeueroeras/Parodontoceras* beds with Mexican and Californian beds with morphologically similar fauna where also occur calpionellids and *Buchia* representatives. A modern systematic revision of this ammonite fauna has not yet been conducted and the absence so far of calpionellids or *Buchia*-like bivalves in the studied section prevents any conclusive correlation.

Finally, major advances have been made in the knowledge of the Tithonian–Berriasian ammonites in the Andes following the work of Aguirre-Urreta et al. (2005), based on new studies of Vennari et al. (2012), Kietzmann and Vennari (2013), Aguirre-Urreta and Vennari (2009), among others (see recent review of Aguirre-Urreta et al., 2011).

In the present study, the traditional assignment of the *Substeueroeras* zone to the topmost Tithonian is maintained. Yet, it should be noted that the first occurrence of *N. kamptneri minor*, which defines the base of the Berriasian, is 4.5 m below the top of the *S. koeneni* zone. This finding may offer a solid argument for its extension to the earliest Berriasian, although the extension to the early Middle Berriasian is not supported by the available evidence.

4.3. U–Pb data

Zircons from a conspicuous 10 cm thick ash-fall tuff (Fig. 3) interbedded with Early Berriasian ammonites bearing sediments were dated by the U–Pb technique using SHRIMP. The dates were confirmed by high-precision U–Pb TIMS analyses of the same zircon population. Zircon grains comprise a homogeneous population formed by stubby crystals with concentric zoning evidenced by cathodoluminescence images. Most of the analyses are concordant, and the SHRIMP data yielded a mean ^{206}Pb – ^{238}U age of 137.9 ± 0.9 Ma (95% confidence, including standard calibration uncertainties) and an intercept age of 138.2 ± 0.7 Ma (2σ) in the Tera–Wasserburg diagram (Fig. 8a). The single-crystal TIMS data from 5 concordant zircon analyses yielded the

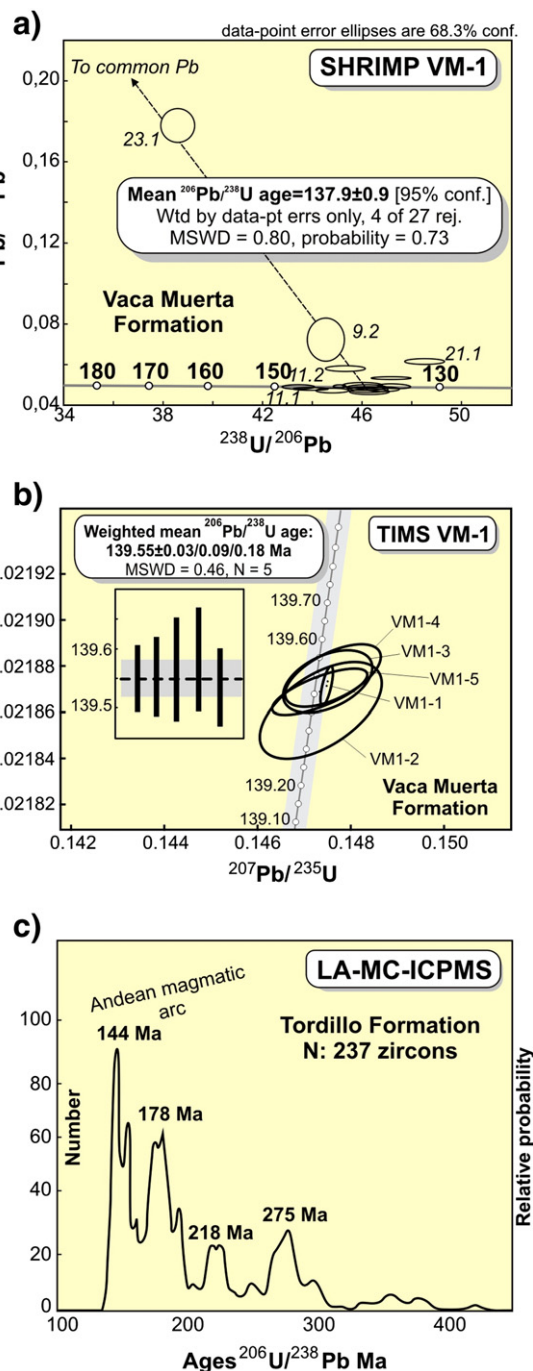


Fig. 8. a) U–Pb SHRIMP ages of zircons from sample VM-1; b) U–Pb TIMS ages of the same zircons; c) LA-MC-ICPMS ages of detrital zircons from Tordillo Formation samples. Analytical data in supplementary information.

precise age of $139.6 \pm 0.09/0.18$ Ma (including systematic errors related to spike calibration and U-decay constant uncertainties) (Fig. 8b). The SHRIMP mean age is somewhat younger than the TIMS age, suggesting that chemical abrasion on the TIMS dates eliminated the effect of a small degree of partial loss of radiogenic lead. Both dates indicate an age between 139.6 and 138.2 Ma for the Early Berriasian in the study section.

The provenance patterns of several sandstone samples of the Tordillo Formation, which underlies the Vaca Muerta Formation, were investigated along the western border of the Neuquén Basin (Fig. 8c). Detrital zircon grains in samples from six localities distributed along hundreds of kilometers were dated by the U–Pb technique using laser-

ablation multi-collector inductively-coupled plasma mass spectrometry (LA–MC–ICPMS), producing 237 concordant ages. They show a statistically robust youngest age peak at ~144 Ma (Naipauer et al., 2012, in press). The red sandstones of the Tordillo Formation, a well studied unit on sedimentological grounds (Spalletti and Piñol, 2005; Veiga and Spalletti, 2007), have traditionally been assigned to the Kimmeridgian–Early Tithonian based on their stratigraphic position beneath the Tithonian fossiliferous marine shales. These shales contain ammonites of the *Virgatosphinctes mendozanus* biozone of late Early Tithonian age (Leanza, 1980; Riccardi, 2008). The obtained ages place the Kimmeridgian–Tithonian boundary at approximately 145 Ma. This maximum age is more than 7 Ma younger than the base of the Tithonian stage (152.1 ± 0.9 Ma, Gradstein et al., 2012; International Stratigraphic Chart, 2012), and may be even younger than the top of the Tithonian stage.

5. Discussion and implications

The present knowledge of the biostratigraphic, chronologic, and geologic data, together with an evaluation of the sedimentary rates in this sector of the Andes, can be interpreted in two contrasting alternatives. The first one accepts the present stage boundary age (Gradstein et al., 2012), and evaluates the data on this framework. The second alternative, mainly based on our local data, proposes new constraints to the J–K boundary and suggests that an age of 140 Ma is the most appropriate boundary age between the Jurassic and Cretaceous.

5.1. A–J–K boundary at 145 Ma

The very precise CA–ID–TIMS age of $139.6 \pm 0.09/0.18$ Ma for the ash-bed in the Vaca Muerta Formation corresponds in the present geological time table to an early Valanginian age. The dated tuff is about 22 m above the first occurrences of *Nannoconus kampteri minor* and *N. steinmanni minor*, two first order nannofossil markers that according to Wimbledon et al. (2011) are used to define the base of the Berriasian. These markers are a few meters above the first occurrence of *N. wintereri*, another biomarker of the top of the Tithonian. If we assume the Andean sedimentation rates computed in the sequence, the ash-bed will be only 0.5 Ma above the boundary. But if we accept that some important hiatuses may exist in this part of the Vaca Muerta Formation, and if we used the late Tithonian sedimentation rate that is derived entirely from the succession of nannofossil first occurrences correlated with the Tethys, the difference could be even larger and close to 3 Ma. In partial support of that interpretation, the ash-bed is 18 m above the top of the *Substeuroceras koeneni* zone. This ammonite zone, although basically Tithonian, may reach the early Berriasian (Riccardi, 2008; Zeiss and Leanza, 2010). This alternative required a late Berriasian age for the dated fossiliferous level and would agree with the present geological time scale.

The drawback of this interpretation is that the dated tuff is in the *Argentinerias noduliferum* zone and below the *S. damesi* zone, which are considered early and late Berriasian in age, based on their correlation with *Subthurmania occitanica* and *S. boissieri* of the Mediterranean zones (see Fig. 6) (Aguirre-Urreta et al., 2011). The Valanginian ammonoids of the Neuquén Basin show strong correlations with those of the classic Mediterranean zones; being especially important the presence of common species of *Olcostephanus*, *Karakaschicerias* and *Neohoplaceras* (Aguirre-Urreta, 1998; Aguirre-Urreta et al., 2008a, 2011).

A late Berriasian or even early Valanginian age of the studied section is difficult to assume because about 10 m above the dated tuff we have found in-situ *Spiticeras* and *Neocosmoceras* of the *Spiticeras damesi* zone. These late Berriasian ammonite genera are well known from the Tethys (Djanélidzé, 1922; Mazonot, 1939; Le Hégarat, 1973). The abundance of berriellids in the analyzed interval of the Las Loicas section, represented by several *Berriasella* species and *Argentinerias* (derived from *Berriassellinae*, according to Wright et al., 1996), also rules out the

possibility of a Valanginian age to this assemblage. It may correspond to the “second faunistic renovation” of Tavera et al. (1986) which takes place after the dominance of *Substeuroceras* species in the precedent *S. koeneni* zone, which has been partially correlated by Olóriz and Tavera (1989) with the final part of Durangites zone of the Mediterranean province.

The 144 Ma age obtained by Naipauer et al. (in press) in the Tordillo Formation, a few meters beneath the base of the Vaca Muerta Formation would indicate, if correct, that both units should be Berriasian in age. This assumption is in a strong discrepancy with the Tithonian age assumed by all the paleontological studies on ammonites of this unit (Leanza, 1980, 1981; Riccardi, 2008; Riccardi et al., 1992, 2000; Zeiss and Leanza, 2010, among many others).

Undoubtedly, more ages near the proposed boundary are necessary to confirm or disregard this alternative.

5.2. A–J–K boundary at 140 Ma

This alternative, which the authors favor based on the present data, has some advantages and some minor drawbacks.

The maximum age of the Vaca Muerta Formation is constrained in 144 Ma, based on the younger frequency peak of detrital zircon dated by U–Pb LA–MC–ICPMS of the underlying Tordillo Formation (Naipauer et al., in press).

The dated tuff layer is located 194 m above the base of Vaca Muerta Formation. Based on the precise age of 139.6 ± 0.2 Ma and the black shales thickness, a maximum local sedimentation rate of 4.41 cm/ka is obtained assuming no major hiatuses in the succession. Recently, Kietzmann et al. (2011) presented cyclostratigraphic studies of Vaca Muerta Formation in the Arroyo Loncoche section some 50 km north-east of the Las Loicas. They recognized 251 elementary cycles of about 20,000 years each for a 215 m thickness of the whole Tithonian. Based on these data, an average sedimentation rate of 4.28 cm/ka can be obtained, which is very close to our computed rate established by very different premises. Assuming either sedimentation rate, and taking in account that the dated tuff is 22.1 m above the nannofossil biostratigraphic J–K boundary (Fig. 3), an estimated age of 140 Ma may be proposed for the Jurassic–Cretaceous boundary in the High Andes.

It is worth mentioning here that thicknesses of the whole Tithonian along the foothills of the Andes in southern Mendoza vary in the platform from 170 to 220 m (Gulisano and Gutiérrez Pleimling, 1994a; Kietzmann et al., 2011), but it is even three to four times thicker to the west and south in central Neuquén Basin where the basinal facies can reach over 1000 m (Leanza, 1973; Leanza and Hugo, 1977; Gulisano and Gutiérrez Pleimling, 1994b).

The main drawback for this assertion is the accepted age for the base of the Berriasian, supported by the 145 Ma age of the Shasky Rise in the Pacific Ocean. However, the biostratigraphic control of this level is very poor by the present nannofossil standards, as reported by Bown (2005). The radiometric Ar–Ar dating, even if only the best two samples were considered, have reduced plateaux that indicate some ^{39}Ar recoil (Mahoney et al., 2005). The ages of these samples are 144.8 ± 1.2 , 143.7 ± 3.0 , and 142.2 ± 5.3 Ma, but 145 Ma was the preferred age as it coincides with the spreading rate assumed for this part of the Pacific Ocean floor (Ogg and Hinnov, 2012).

A brief review of the J–K boundary history in the past 50 years shows that this boundary has varied from 130 to 145 Ma because of the varying assumptions used. Estimates based on K–Ar dating of glauconite in the earliest Cretaceous sandstones and assuming equal duration of the ammonite biozones were between 130 and 135 Ma (Odin, 1982, 1994). Estimates mainly based on the ammonite zones scaled according to their calibration to the magnetic polarity time scale, assuming a constant Pacific spreading rate indicate a much older boundary at 145 Ma (Gradstein et al., 2004, 2012). Although there is consensus that U–Pb dating of ash-fall tuffs with good biostratigraphic

control is more reliable (Pálffy, 2008), the scarcity of this type of data in the classic Tethyan sections, where there are not tuffs, meant that precise dating of the Jurassic–Cretaceous boundary remained elusive. One of the few contributions based on U–Pb zircon data in ash-fall tuffs obtained an age of 137.1 ± 0.6 Ma assigned to the late Berriasian for a tuff from the Great Valley sequence of Northern California (Bralower et al., 1990). The biostratigraphic control was based on the zonation of different species of the bivalve *Buchia* and nannofossil markers. These authors proposed that the J–K boundary should be at 141.5 Ma on the basis of an assumed duration of the Berriasian. However, this high-precision age was disregarded by other authors (Gradstein et al., 1994), who argued that the ages of the mollusk and nannofossil assemblages were not sufficiently precise and reliable at that time.

The age of 137.1 ± 0.6 Ma for the late Berriasian in California (Bralower et al., 1990) and our age of 139.6 ± 0.2 Ma for the base of the Berriasian are highly coherent. The latter makes it possible to constrain the J–K boundary at approximately 140 Ma.

The U–Pb ages of the Tordillo Formation based on detrital zircons may not be as accurate as the TIMS and SHRIMP data but they do provide further constraints to the age of the basal Tithonian. The present Kimmeridgian–Tithonian boundary has been accepted to be at 152.1 Ma, but the maximum age of the Tordillo Formation sandstones is 144 Ma. These sandstones underlie the Vaca Muerta deposits, where ammonites of the *Virgatosphinctes mendozanus* biozone are present. The base of this zone has been correlated with the Darwini standard zone of the Tethys (Riccardi et al., 2000; Riccardi, 2008), which corresponds to the middle part of the chron M22 (Ogg and Hinnov, 2012). Based on this correlation, we propose that the base of the Tithonian should be younger than 145 Ma.

Our proposed ages to the Andean J–K boundary and the base of the Tithonian are consistent, despite the ages being obtained from two different and independent data sets, robust U–Pb SHRIMP and TIMS data from volcanic zircons at the base of the Berriasian and a large database of detrital zircons (237 concordant ages) measured by LA–MC–ICPMS for the early Tithonian. These results are also consistent with another U–Pb SHRIMP age (132.5 ± 1.3 Ma) obtained from an ash-fall tuff for a well-constrained Hauterivian ammonite assemblage of the Agrio Formation in the Neuquén Basin (Aguirre-Urreta et al., 2008b).

These new data indicate that either the dated fossiliferous bed is late Berriasian and the whole ammonite zonation should be changed, or that the base of the Berriasian is close to 139.6 ± 0.2 Ma. Based on the sedimentation rate and our confidence in the local biozones we propose a 140 Ma old J–K boundary in the Andean basins of Western Gondwana as the best alternative. Our data also indicate that the base of the Tithonian may be younger than 145 Ma.

Acknowledgments

We would like to thank Leonardo Legarreta for sharing with us his knowledge of the Neuquén Basin and Martín Hoquí and Ramiro Ezquerro for field assistance. Special thanks to James Ogg and Jozsef Palfy for constructive comments and reviews in an earlier version of this manuscript. This is contribution R-95 of the Instituto de Estudios Andinos Don Pablo Groeber (UBA-CONICET).

Appendix A. Supplementary data

Supplementary data to this article can be found online at <http://dx.doi.org/10.1016/j.gr.2013.07.005>.

References

Aguirre-Urreta, M.B., 1998. The ammonites *Karakaschicerias* and *Neohoplaceras* (Valanginian Neocomitidae) from the Neuquén Basin, west-central Argentina. *Journal of Paleontology* 72, 39–59.

- Aguirre-Urreta, M.B., Rawson, P.F., 1997. The ammonite sequence in the Agrio Formation (Lower Cretaceous), Neuquén basin, Argentina. *Geological Magazine* 134, 449–458.
- Aguirre-Urreta, B., Vennari, V., 2009. On Darwin's footsteps across the Andes: Tithonian–Neocomian fossil invertebrates from the Piuquenes Pass. *Revista de la Asociación Geológica Argentina* 64, 32–42.
- Aguirre-Urreta, M.B., Rawson, P.F., Concheyro, G.A., Bown, P.R., Ottone, E.G., 2005. Lower Cretaceous Biostratigraphy of the Neuquén Basin. In: Veiga, G., Spalletti, L., Howell, J.A., Schwarz, E. (Eds.), *The Neuquén Basin: A Case Study in Sequence Stratigraphy and Basin Dynamics*. Geological Society, London, Special Publication, 252, pp. 57–81.
- Aguirre-Urreta, M.B., Mourgues, F.A., Rawson, P.F., Bulot, L.G., Jaillard, E., 2007. The Lower Cretaceous Chañarillo and Neuquén Andean basins: ammonoid biostratigraphy and correlations. *Geological Journal* 42, 143–173.
- Aguirre-Urreta, M.B., Casadio, S., Cichowski, M., Lazo, D.G., Rodríguez, D., 2008a. Afinidades paleobiogeográficas de los invertebrados cretácicos de la cuenca Neuquina. *Ameghiniana* 45, 593–613.
- Aguirre-Urreta, M.B., Pazos, P.J., Lazo, D.G., Fanning, C.M., Litvak, V.D., 2008b. First U–Pb SHRIMP age of the Hauterivian stage, Neuquén Basin, Argentina. *Journal of South American Earth Sciences* 26, 91–99.
- Aguirre-Urreta, B., Lazo, D.G., Griffin, M., Vennari, V., Parras, A.M., Cataldo, C., Garberoglio, R., Luci, L., 2011. Megainvertebrados del Cretácico y su importancia bioestratigráfica. In: Leanza, H.A., Arregui, C., Carbone, O., Danieli, J.C. (Eds.), *Geología y Recursos Naturales del Neuquén*. Asociación Geológica Argentina, Buenos Aires, pp. 465–488.
- Ballent, S.C., Ronchi, D.I., Angelozzi, G., 2004. Microfósiles calcáreos tithonianos (Jurásico superior) en el sector oriental de la Cuenca Neuquina, Argentina. *Ameghiniana* 41, 13–24.
- Bornemann, A., Aschwer, U., Mutterlose, J., 2003. The impact of calcareous nannofossils on the pelagic carbonate accumulation across the Jurassic/Cretaceous boundary. *Palaeogeography, Palaeoclimatology, Palaeoecology* 199, 187–228.
- Bown, P.R., 2005. Early to mid-Cretaceous calcareous nannoplankton from the northwest Pacific Ocean, ODP Leg 198, Shatsky Rise. In: Bralower, T.J., Premoli Silva, I., Malone, M.J. (Eds.), *Proceedings Ocean Drilling Program, Scientific Results*, 198 (Online), <http://www-dp.tamu.edu/publications/198_SR/103/103.htm>.
- Bown, P., Concheyro, A., 2004. Lower Cretaceous calcareous nannoplankton from the Neuquén Basin, Argentina. *Marine Micropaleontology* 52, 51–84.
- Bowring, S.A., Erwin, D., Parrish, R., Renne, P., 2005. EARTHTIME: a community-based effort towards high-precision calibration of earth history. *Geochimica et Cosmochimica Acta* 69, A316.
- Bralower, T.J., Monechi, S., Thierstein, H.R., 1989. Calcareous nannofossil zonation of the Jurassic–Cretaceous boundary interval and correlation with the geomagnetic polarity timescale. *Marine Micropaleontology* 14, 153–235.
- Bralower, T.J., Ludwig, K.R., Obradovich, J.D., Jones, D.L., 1990. Berriasian (Early Cretaceous) radiometric ages from the Grindstone Creek Section, Sacramento Valley, California. *Earth and Planetary Science Letters* 98, 62–73.
- Cantú-Chapa, A., 2006. New Upper Tithonian (Jurassic) ammonites of the Chinameca Formation in Southern Veracruz, Eastern Mexico. *Journal of Paleontology* 80, 294–308.
- Casellato, C., 2009. Causes and Consequences of Calcareous Nannoplankton Evolution in the Late Jurassic: Implications for Biogeochronology, Biocalcification and Ocean Chemistry. (Ph.D. thesis) Università degli Studi di Milano.
- Casellato, C.E., 2010. Calcareous nannofossil biostratigraphy of Upper Callovian–Lower Berriasian from the Southern Alps, North Italy. *Rivista Italiana di Paleontologia e Stratigrafia* 116, 357–404.
- Channell, J.E.T., Casellato, C.E., Muttoni, G., Erba, E., 2010. Magnetostratigraphy, nannofossil stratigraphy and apparent polar wander for Adria–Africa in the Jurassic–Cretaceous boundary interval. *Palaeogeography, Palaeoclimatology, Palaeoecology* 293, 51–75.
- Checa, A., 1985. Los aspidoceratiformes en Europa (Ammonitina, Fam. Aspidoceratidae: Subfamilias Aspidoceratinae y Physodoceratinae). (Tesis Doctoral) Universidad de Granada 1–413.
- Concheyro, A., Angelozzi, G., Ronchi, D., 2007. Microfósiles calcáreos del límite Jurásico–Cretácico de la cuenca Neuquina. Tercer Simposio Argentino del Jurásico, Mendoza, Actas, p. 34.
- de Kaenel, E., Bergen, J.A., 1996. Mesozoic calcareous nannofossil biostratigraphy from Sites 897, 899, and 901, Iberia Abyssal Plain: new biostratigraphic evidence. In: Whitmarsh, R.B., Sawyer, D.S., Klaus, A., Masson, D.G. (Eds.), *Proceedings Ocean Drilling Program, Scientific Results*, 149, pp. 27–59.
- Djanéidzé, M.A., 1922. Les *Spiticeras* du sud-est de la France. Mémoires pour servir à l'explication de la carte géologique détaillée de la France. Contributions à l'étude des céphalopodes paléocrétacés du sud-est de la France (matériaux pour servir à la connaissance du crétacé inférieur) Impr. Nationale, Paris (207 pp.).
- Gerstenberger, H., Haase, G., 1997. A highly effective emitter substance for mass spectrometric Pb isotope ratio determinations. *Chemical Geology* 136, 309–312.
- Gerth, E., 1921. Fauna und Gliederung des Neokoms in der argentinischen Cordillere. Zentralblatt für Mineralogie, Geologie und Paläontologie 1921 (112–119), 140–148.
- Gradstein, F.M., Agterberg, F., Ogg, J., Hardenbol, J., van Veen, P., Thierry, J., Huang, Z., 1994. A Mesozoic time scale. *Journal of Geophysical Research* 99, 24051–24074.
- Gradstein, F.M., Ogg, J.G., Smith, A., 2004. *A Geologic Time Scale*. Cambridge University Press, Cambridge (589 pp.).
- Gradstein, F.M., Ogg, J.G., Schmitz, M.D., Ogg, G.M. (Eds.), 2012. *The Geologic Time Scale 2012*. Elsevier, China (1144 pp.).
- Gulisano, C.A., Gutiérrez Pleimling, A., 1994a. Field guide to the Jurassic of the Neuquén Basin, province of Mendoza. Secretaría de Minería de la Nación, Dirección Nacional del Servicio Geológico, Publicación, 159 1–103.
- Gulisano, C.A., Gutiérrez Pleimling, A., 1994b. Field guide to the Jurassic of the Neuquén Basin, province of Neuquén. Secretaría de Minería de la Nación, Dirección Nacional del Servicio Geológico, Publicación, 158 1–111.

- Gulisano, C.A., Gutiérrez Pleimling, A.R., Digregorio, R.E., 1984. Análisis estratigráfico del intervalo Tithoniano Valanginiano (Formaciones Vaca Muerta, Quintuco y Mulichinco) en el suroeste de la provincia del Neuquén. 9 Congreso Geológico Argentino, Actas, 1, pp. 221–235.
- International Stratigraphic Chart, 2012. International Commission of Stratigraphy: IUGS-UNESCO. <http://www.stratigraphy.org/column.php?id=Chart/TimeScale>.
- Jordan, T., Isacks, B., Ramos, V.A., Allmendinger, R.W., 1983. Mountain building model: the Central Andes. *Episodes* 1983 (3), 20–26.
- Kessel, K., Mutterlose, J., Michalzik, D., 2006. Early Cretaceous (Valanginian–Hauterivian) calcareous nannofossils of the northern hemisphere: a key group for the understanding of Cretaceous climate. *Lethaia* 39, 157–172.
- Kietzmann, D., Vennari, V., 2013. Sedimentología y estratigrafía del límite Jurásico–Cretácico de la Cuenca Neuquina en el área del Cerro Domuyo, norte de Neuquén, Argentina. *Andean Geology* 40, 41–65.
- Kietzmann, D., Martín Chivelet, J., Palma, R., López Gómez, J., Lescano, M., Concheyro, A., 2011. Evidence of precessional and eccentricity orbital cycles in a Tithonian source rock: the mid-outer carbonate ramp of the Vaca Muerta Formation, northern Neuquén Basin, Argentina. *Bulletin of the American Association of Petroleum Geologists* 95, 1459–1474.
- Le Hégarat, G., 1973. Le Berriasien du Sud-East de la France. *Documents des Laboratoires de Géologie de Lyon* 43, 1–309.
- Leanza, A.F., 1945. Ammonites del Jurásico Superior y del Cretácico Inferior de la Sierra Azul, en la parte meridional de la provincia de Mendoza. *Anales del Museo de La Plata NS* 1, 1–99.
- Leanza, H.A., 1973. Estudio sobre los cambios faciales de los estratos limítrofes Jurásico–Cretácicos entre Loncopué y Picún Leufú, Prov. del Neuquén, Rep. Argentina. *Revista de la Asociación Geológica Argentina* 18, 97–132.
- Leanza, H.A., 1980. The Lower and Middle Tithonian ammonite fauna from Cerro Lotena, Province of Neuquén, Argentina. *Zitteliana* 5, 3–49.
- Leanza, H.A., 1981. The Jurassic–Cretaceous boundary beds in West Central Argentina and their ammonite zones. *Neues Jahrbuch für Geologie und Paläontologie, Abhandlungen* 161, 62–92.
- Leanza, H.A., 1996. Advances in the ammonite zonation around the Jurassic/Cretaceous boundary in the Andean Realm and correlation with Tethys. *Jost Wiedmann Symposium, Tübingen, Abstracts*, pp. 215–219.
- Leanza, H.A., Hugo, C., 1977. Sucesión de ammonites y edad de la Formación Vaca Muerta y sincrónicas entre los paralelos 35° y 40° LS. Cuenca Neuquina–Mendocina. *Revista de la Asociación Geológica Argentina* 32, 248–264.
- Legarreta, L., Uliana, M.A., 1991. Jurassic–Cretaceous marine oscillations and geometry of back-arc basin fill, central Argentine Andes. *International Association of Sedimentology, Special Publication* 12, 429–450.
- Legarreta, L., Uliana, M.A., 1999. El Jurásico y Cretácico de la Cordillera Principal y la Cuenca Neuquina. 1. Facies sedimentarias. In: Caminos, R. (Ed.), *Geología Argentina*. Instituto de Geología y Recursos Minerales, Buenos Aires, pp. 399–416.
- Mahoney, J.J., Duncan, R.A., Tejada, M.L.G., Sager, W.W., Bralower, T.J., 2005. Jurassic–Cretaceous boundary age and mid-ocean-ridge-type mantle source for Shatsky Rise. *Geology* 33, 185–188.
- Matteini, M., Junges, S.L., Dantas, E.L., Pimentel, M.M., Bühn, B., 2010. In situ zircon U–Pb and Lu–Hf isotope systematic on magmatic rocks: insights on the crustal evolution of the Neoproterozoic Goiás Magmatic Arc, Brasília belt, Central Brazil. *Gondwana Research* 17, 1–12.
- Mattinson, J., 2005. Zircon U–Pb chemical abrasion (“CA–TIMS”) method: combined annealing and multi-step partial dissolution analysis for improved precision and accuracy of zircon ages. *Chemical Geology* 220, 47–66.
- Mazenot, G., 1939. Les Palaeohoplitidae Tithoniques et Berriasiens du Sud-Est de la France. *Mémoires de la Société Géologique de France* 18 (1–4), 1–303.
- McLean, N.M., Bowring, J.F., Bowring, S., 2011. An algorithm for U–Pb isotope dilution data reduction and uncertainty propagation. *Geochemistry, Geophysics, Geosystems* 12, Q0AA18. <http://dx.doi.org/10.1029/2010GC003478>.
- Michálik, J., Reháková, D., 2011. Possible markers of the Jurassic/Cretaceous boundary in the Mediterranean Tethys: a review and a state of art. *Geoscience Frontiers* 2, 475–490.
- Naipauer, M., García Morabito, E., Marques, J.C., Tunik, M., Rojas Vera, E., Vujovich, G.I., Pimentel, M., Ramos, V.A., 2012. Intraplate Late Jurassic deformation and exhumation in western central Argentina: constraints from surface data and U–Pb detrital zircon ages. *Tectonophysics* 524–525, 59–75.
- Naipauer, M., Tunik, M., Marques, J.C., Rojas Vera, E.A., Vujovich, G.I., Pimentel, M.M., Ramos, V.A., 2013. U–Pb detrital zircon ages of Upper Jurassic continental successions: implications for the provenance and absolute age of the Jurassic–Cretaceous boundary in the Neuquén Basin. In: Sepúlveda, S., Giambiagi, L., Pinto, L., Moreiras, S., Tunik, M., Hoke, G., Fariás, M. (Eds.), *Geodynamic Processes in the Andes of Central Chile and Argentina*. Geological Society, Special Publication (London, in press).
- Odin, G.S., 1982. Numerical Dating in Stratigraphy. John Wiley & Sons, Chichester (1094 pp.).
- Odin, G.S., 1994. Geologic time scale. *Comptes Rendus de l'Académie des Sciences de Paris, Série II* 318, 59–71.
- Ogg, J.G., 2004. The Jurassic period. In: Gradstein, F., Ogg, J.G., Smith, A.G., et al. (Eds.), *A Geologic Time Scale*. Cambridge University Press, Cambridge, pp. 307–343.
- Ogg, J.G., Hinnov, L.A., 2012. The Jurassic period. In: Gradstein, F., Ogg, J.G., Schmitz, M.D., Ogg, G.M. (Eds.), *The Geologic Time Scale 2012*. Elsevier, China, pp. 731–791.
- Ogg, J.G., Ogg, G., Gradstein, F.M., 2008. *The Concise Geologic Time Scale*. Cambridge University Press (177 pp.).
- Olóriz, F., Tavera, J.M., 1989. The significance of Mediterranean ammonites with regard to the traditional Jurassic–Cretaceous boundary. *Cretaceous Research* 10, 221–237.
- Pálffy, J., 1995. Development of the Jurassic geochronologic scale. *GECZY Jubilee Volume, Hantkeniana* 1, 13–25.
- Pálffy, J., 2008. The quest for refined calibration of the Jurassic time-scale. *Proceedings of the Geologists' Association* 119, 85–95.
- Ramos, V.A., Folguera, A., 2005. Tectonic evolution of the Andes of Neuquén: constraints derived from the magmatic arc and foreland deformation. In: Veiga, G., Spalletti, L.A., Howell, J.A., Schwarz, E. (Eds.), *The Neuquén Basin: A Case Study in Sequence Stratigraphy and Basin Dynamics*. The Geological Society, Special Publication, 252, pp. 15–35.
- Rawson, P.F., 2000. Cretaceous. In *Explanatory note to the International Stratigraphic Chart*. Division of Earth Sciences, UNESCO.
- Reboullet, S., Rawson, P.F., Moreno-Bedmar, J.A., Aguirre-Urreta, M.B., Barragan, R., Bogomolov, Y., Company, M., Gonzalez-Arreola, C., Stoyanova, V.I., Lukeneder, A., Matrión, B., Mitta, V., Randrianaly, H., Vasicek, Z., Baraboshkin, E.J., Bert, D., Bersac, S., Bogdanova, T.N., Bulot, L.G., Latil, J.-L., Mikhailova, I.A., Ropolo, P., Szives, O., 2011. Report on the 4th International Meeting of the IUGS Lower Cretaceous Ammonite Working Group, the “Kilian Group” (Dijon, France, 30th August 2010). *Cretaceous Research* 32, 786–793.
- Riccardi, A.C., 1988. The Cretaceous System of southern South America. *Memoir Geological Society of America* 168, 1–161.
- Riccardi, A.C., 1991. Jurassic and Cretaceous marine connections between the south-east Pacific and Tethys. *Palaeogeography, Palaeoclimatology, Palaeoecology* 87, 155–189.
- Riccardi, A.C., 2008. The marine Jurassic of Argentina: a biostratigraphic framework. *Episodes* 31, 326–335.
- Riccardi, A.C., Gulisano, C.A., Mojica, J., Palacios, O., Schubert, C., Thomson, M.R.A., 1992. Western South America and Antarctica. In: Westermann, G.E.G. (Ed.), *The Jurassic of the Circum Pacific*. Cambridge University Press, Cambridge, pp. 122–161.
- Riccardi, A.C., Leanza, H.A., Damborenea, S.E., Manceñido, M.O., Ballent, S.C., Zeiss, A., 2000. Marine Mesozoic biostratigraphy of the Neuquén Basin. *Zeitschrift für Angewandte Geologie* 1, 103–108.
- Scasso, R., Concheyro, A., 1999. Nanofósiles calcáreos, duración y origen de ciclos calizamarra (Jurásico tardío de la Cuenca Neuquina). *Revista de la Asociación Geológica Argentina* 54, 290–297.
- Spalletti, L.A., Piñol, F.C., 2005. From alluvial fan to playa: an upper Jurassic ephemeral fluvial system, Neuquén Basin, Argentina. *Gondwana Research* 8, 363–383.
- Tavera, J.M., Checa, A., Olóriz, F., Company, M., 1986. Mediterranean ammonites and the Jurassic–Cretaceous boundary in Southern Spain (Subbetic Zone). *Acta Geologica Hungarica* 29, 151–159.
- Thierstein, H., 1971. Tentative Lower Cretaceous calcareous nannoplankton zonation. *Eclogae Geologicae Helveticae* 64, 459–488.
- Veiga, G.D., Spalletti, L.A., 2007. The Upper Jurassic (Kimmeridgian) fluvial-aeolian systems of the southern Neuquén Basin, Argentina. *Gondwana Research* 11, 286–302.
- Veiga, G.D., Spalletti, L.A., Howell, J.A., Schwarz, E. (Eds.), 2005. *The Neuquén Basin: a case study in sequence stratigraphy and basin dynamics*. The Geological Society, Special Publication, 252, pp. 1–336.
- Vennari, V.V., Álvarez, P.P., Aguirre-Urreta, B., 2012. A new species of *Andiceras* Krantz (Cephalopoda: Ammonoidea) from the Late Jurassic–Early Cretaceous of the Neuquén Basin, Mendoza, Argentina. *Systematics and Biostratigraphy, Andean Geology* 39, 92–105.
- Williams, I.S., Claesson, S., 1987. Isotopic evidence for the Precambrian provenance Caledonian metamorphism of high grade paragneisses from the Seve Nappes, Scandinavian Caledonides. II ion microprobe zircon U–Th–Pb. *Contributions to Mineralogy and Petrology* 97, 205–217.
- Wimbledon, W.A.P., Casellato, C.E., Reháková, D., Bulot, L.C., Erba, E., Gardin, S., Verreussel, R.M., Munsterman, D.K., Hunt, C.O., 2011. Fixing a basal Berriasian and Jurassic–Cretaceous (J–K) boundary – is there perhaps some light at the end of the tunnel? *Rivista Italiana di Paleontologia e Stratigrafia* 117, 295–307.
- Wright, C.W., Callomon, J.H., Howarth, M.K., 1996. *Cretaceous Ammonoidea. Treatise on invertebrate paleontology. Part L. Mollusca 4 (revised)*. Boulder, Co., Geological Society of America and Lawrence, K.S. University of Kansas Press, Kansas (362 pp.).
- Zeiss, A., 1983. Zur Frage der Äquivalenz der Stufen Tithon/Berrias/Wolga/Portland in Eurasien und Amerika. Ein Beitrag zur Klärung der weltweiten Korrelation der Jura-/Kreide-Grenschichten im marinen Bereich. *Zitteliana* 10, 427–438.
- Zeiss, A., 1986. Comments on a tentative correlation chart for the most important marine provinces at the Jurassic/Cretaceous Boundary. *Acta Geologica Hungarica* 29, 27–30.
- Zeiss, A., Leanza, H.A., 2010. Upper Jurassic (Tithonian) ammonites from the lithographic limestones of the Zapala region, Neuquén Basin, Argentina. *Beringeria* 41, 25–76.